CrystEngComm

Accepted Manuscript

ROYAL SOCIETY OF CHEMISTRY

www.rsc.org/crystengcomm

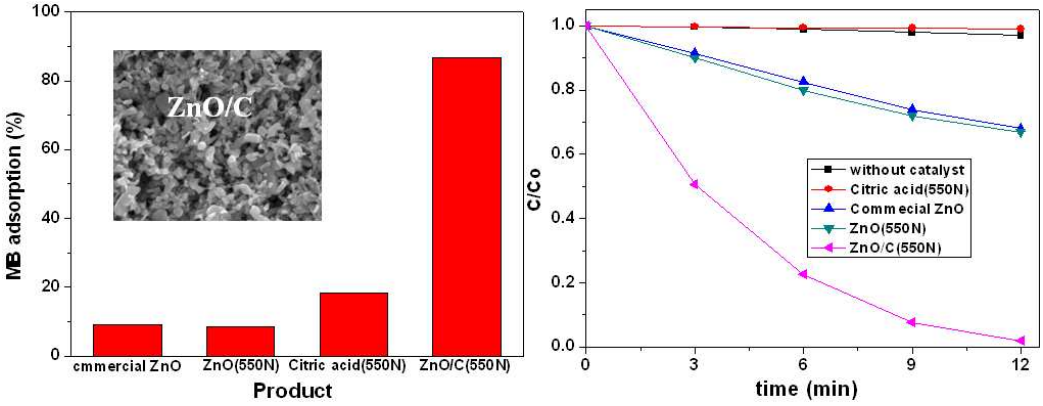

A facile route for the preparation of ZnO/C composites with high photocatalytic activity and adsorption capacity

Shuaishuai Ma‡, Jinjuan Xue‡, Yuming Zhou,* Zewu Zhang, Xin Wu

School of Chemistry and Chemical Engineering, Southeast University, Nanjing 211189, P. R. China

Abstract:

This manuscript describes the deposition of carbon on the surface of ZnO nanoparticles via a simple adsorption and calcination process. The prepared ZnO/C sample was characterized by X-ray diffraction (XRD), scanning electron microscopy (SEM), transmission electron microscopy (TEM), energy-dispersive X-ray (EDS) spectroscopy and thermogravimetric analysis (TGA), the results indicated that the carbon was successfully doped on the surface of the ZnO nanoparticles. The photocatalytic activity and adsorption capacity were evaluated by photocatalytic decomposition and adsorption of the dye methylene blue (MB) in aqueous solution. The results showed that the obtained ZnO/C sample exhibited much higher photocatalytic property and adsorption capacity to MB than the pure ZnO and carbon because of the formation of heteroarchitectures, which might improved the separation of photogenerated electrons and holes. In particular, the psedudo-first-order rate constant of the ZnO/C sample was 0.326 min^{-1} which was 10 times than that of pure ZnO. Moreover, the ZnO/C composites could remove dyes in different water source like Changjiang river water with high efficiency as well as in deionized water and will greatly promote their application in the area of environmental remediation.

* Corresponding author. Tel.: +86 25 52090617; fax: +86 25 52090617.
E-mail address: ymzhou@seu.edu.cn (Yuming Zhou).
‡S.S. Ma and J.J. Xue contributed equally to this work.

Introduction

During the past decades, environmental problems such as air and water pollution have provided the impetus for sustained fundamental and applied research in the area of environmental remediation.[1-3] With the development of nanoscience and nanotechnology, the application of nanostructured semiconductors such as Bi_2O_3, Fe_2O_3, TiO_2 and ZnO, have been developed for creating a comfortable environment for human beings.[4-9] Among these semiconductors, zinc oxide (ZnO) in the area of photocatalysis has grown considerably, due to its physical and chemical stability, high catalytic activity, low cost, environmental friendliness and easy of availability.[10-12] Although notable advances have been made, the high recombination rate of the photogenerated electron/hole pairs hinders its further application in industry. As a result, several attempts have been made to reduce the recombination of photogenerated electron/hole pairs during the photocatalyitc reactions by developing ZnO-based heterostructures or composites with electron scavenging agents such as metals, metal oxides or organic molecules.[13-15] For instance, the combination of ZnO with γ-Fe_2O_3 generated bifunctional materials that possess magnetic and photoluminescent properties simultaneously;[16] the attachment of CdTe and CdSe quantum dots onto ZnO improved the optical adsorption ability toward visible lights of the latter as well as the photovoltaic performance[17] and the epitaxial growth of Ag and Au on ZnO nanoparticles accelerated the separation process of photogenerated electrons and holes in ZnO and increased the photocatalytic activity of ZnO.[18, 19]

It is well known amorphous carbon is widely served as an intercomponent to be deposited on the surface of polymers, ceramics, metals, and oxides in order to modify the

corrosion resistance, thermal stability, adsorbability, or electronic properties of these materials. Especially, fabricating a carbon layer onto the surface of several materials is a conventional method to improve the properties of the materials.[20] If the surface of nanostructured ZnO is modified with carbon, the good properties of ZnO and carbon will be integrated into the hybrids, which is advantageous to overcoming some intrinsic defects of ZnO.[21-23] Recently, carbon materials have been widely used as ideal electron pathways due to their good conductivity. Some results have demonstrated that carbon materials could efficiently capture and transport of photogenerated electrons because of their highly conductive activity. According to the excellent photocatalyst activity of ZnO/C, the combination of ZnO and carbon nanoparticles seems to be an ideal way of hindering the recombination of electrons and holes and improving the photocatalytic efficiency. To date, several studies of C-doped ZnO have been reported. These studies mainly focused on ferromagnetism, magnetotransport properties, and p-type conduction properties of C-doped ZnO, and the synthetic approaches have been based on vapor-phase techniques. However, these techniques generally require expensive equipment, complex process control, and stringent reaction conditions.[24-26]

In this paper, we reported a successful attempt for the fabrication of ZnO/C composites via a simple adsorption and calcination technique method with citric acid as carbon source. This protocol does not need expensive equipment, complex process control, and stringent reaction conditions, and thus is simple and cost-effective. Both the photocatalytic activity and adsorption capacity of ZnO/C composites were investigated by measuring the degradation and adsorption of dye MB as a test substance. The experimental results showed that the as-obtained ZnO/C composites exhibited excellent photocatalytic activity and adsorption

capacity. Moreover, in order to evaluate whether the sample was suitable for practical applications, MB was added in different water sources including tap water and river water collected from Changjiang River in China to form several different MB solutions, and then treated with the as-prepared ZnO/C composites. The results revealed that ZnO/C composites could remove dyes in living water samples with high efficiency as well as in deionized water and will greatly promote their application in the area of environmental remediation.

Experimental section

Preparation of ZnO/C composites

All reagents were of analytical grade and were used as purchased without further purification. In our experiments, the preparing process consisted of two steps. Firstly, 0.2 g of citric acid was dissolved in 5ml of deionized water to form aqueous solution, and then 0.2 g commercial ZnO powder was added into the citric acid solution. Subsequently, the above suspension was treated with ultrasound for 5 min and stirred for another 4 h at room temperature to obtain ZnO-citric acid precursor. After that, the as-prepared precursor was collected and dried at 60 ^{o}C for 12 h. Secondly; the precursor was placed in an annealing furnace and maintained at 550 ^{o}C for 2 h in N_2 atmosphere. After calcination, it was found that the solid product had changed its color from the initial white to brown, suggesting the existence of carbon component in the product. The brown solid sample was collected and washed for several times with distilled water and ethanol, then dried in vacuum at 60 ^{o}C for 4h and marked as ZnO/C (550N). Commercial ZnO and citric acid were treated in the same way as the comparative samples, which were marked as ZnO (550N) and citric acid (550N)

Sample characterizations

The crystal structure and morphologies of the products were characterized by using a combination of the following techniques: X-ray diffraction (XRD, Rigaku Ultima □, Cu Kα radiation), transmission electron microscopy (TEM, JEM-1230) and scanning electron microscope (SEM, JEOL JSM-6510LV) coupled with an energy-dispersive X-ray spectroscopy (EDS, Oxford instruments X-Max). Nitrogen adsorption isotherms at liquid nitrogen temperature (77K) were measured with a Micromeritics ASAP 2020 (Micromertics USA) static volumetric gas adsorption instrument. The specific surface area was determined from the linear part of the BET equation. Thermogravimetric analysis (TGA) of the samples were performed with a Rigaku ThermoPlus TG8120 system from room temperature to 800 ^{o}C at a heating rate of 10 ^{o}C•min^{-1} under oxygen or argon. PL properties were measured using room temperature photoluminescence with a 325 nm He-Cd laser excitation wavelength (Shimadzu RF-5301).

Adsorption and photocatalytic decomposition of MB

A MB solution with a concentration of 30 mg/L was prepared by dissolving the dye in distilled water. 20 mg of the sample was dispersed into the MB solution (100 mL) in a cylindrical glass jacketed reactor equipped with reflux water to keep the reaction temperature constant. The resultant mixture was stirred in the dark for a fixed time to evaluate the adsorption capacity. The concentration of MB was analyzed using a UV-3600 (Shimadzu) spectrometer, and the time-dependent absorption at 664 nm was recorded.

The photocatalytic decomposition of MB was studied using the prepared MB stock solution. After stirring in the dark for a fixed time to reach adsorption-desorption equilibrium.

The suspension was exposed to UV irradiation (250 W, GY-250, λ=365nm) with stirring. During the process of photodegradation, 3 mL of the suspension was sampled every three minutes and the supernatant was kept for UV-vis characterization to determine the contents of MB after centrifugation.

Results and discussion

Structure and morphology of the products

The structure of ZnO/C (550N) was characterized by X-ray diffraction (XRD, Fig. 1 (a)), and as a comparison, the XRD pattern of commercial ZnO was also included. As can be seen, all the diffraction peaks of ZnO/C (550N) in Fig. 1 (a) can be indexed to ZnO in a hexagonal structure; their strong and sharp features suggested that ZnO/C (550N) was still well crystalline, which was similar with the commercial ZnO. Meanwhile, the carbonaceous species of the ZnO/C (550N) were confirmed to be amorphous phases due to the absence of a reflection at 26^{o}-28^{o}, which is the typical peak of crystalline graphitic layers of carbonaceous materials. In addition, the EDX pattern (Fig. 1 (b)) also indicated that the structures were only composed of Zn, O, and C.

The morphology of the as-prepared ZnO/C (550N) sample was observed by SEM and TEM analysis. Fig. 2 (a and b) show the typical SEM images of the as-prepared ZnO/C (550N) sample. From Fig. 2 (a and b), it can be observed the particle size of the ZnO/C (550N) sample is distribute in a wide range of dimensions. The TEM analysis was further employed to gain more information about the composites structure. As illustrated in Fig. 2 (c, d), the amorphous carbonaceous layer can be obviously distinguished and the presence of transparent

layers in the as-prepared ZnO/C (550N) product indicating the carbonaceous layers with a low electron density. In addition, the transparency of the carbon substrate also suggested that the obtained product had a high porosity.

The thermal property of the ZnO/C (550N) was further characterized by thermogravimetric (TGA) analysis. As shown in Fig. 3 (a), two main weight loss events were observed in the TGA curve. The first one that occurred between room temperature and 150 ^{o}C with a weight loss of about 1 wt% should be attributed to the desorption of physically adsorbed water from the sample. Another weight loss of 14 wt% occurred between 400 ^{o}C and 550 ^{o}C due to the combustion of the carbon layer. In order to investigate the utilization of citric acid in the calcination process, a preview report about the thermal transformations of citric acid is shown in Fig. 3 (b).[27] According to the preview report, the weight loss of citric acid below 100 ^{o}C is mainly ascribed to water loss. Citric acid melts at 153 ^{o}C and dehydrates to give aconitic acid on heating at 175 ^{o}C. Further heating at about 220 ^{o}C results in the formation of methyl maleic anhydride through decarboxylation.[28] This is a complex process leading through dehydration and decarboxylation reactions to different intermediate products. Due to similar structural features of the intermediate products, their identification is fairly difficult. The analysis of the volatiles using mass spectrometry revealed ions at m/z 39 and 68 in each case. However, they are characteristic of both the itaconic and citraconic anhydride. On the other hand, the IR spectra reveal that the product is cyclic acid anhydrides and suggest that the final decomposition product is itaconic and/or citraconic anhydride.[27] As we can see in Fig 3 (b), citric acid transform into itaconic anhydride and citraconic anhydride through dehydration and decarboxylation at last. In our experiment, the dosage of citric acid was 0.2 g,

after the thermal transformation, about 0.05g itaconic anhydride and citraconic anhydride could be obtained. Thus, the theoretical weight ratio of carbon particles on the ZnO surface was about 20 wt% by calculation, which was higher than the actual carbon weight ratio. This phenomenon is probably attributed to the loss and incomplete absorption during the experiment process.

The nitrogen adsorption-desorption isotherm of ZnO/C (550N) is shown in Fig. 4. The shape of the nitrogen isotherms resemble a combined type I/IV isotherm: a steep increase at low relative pressure and the following small slope at intermediate relative pressure occurred concomitantly with the desorption hysteresis, revealing the presence of a combination of micropores (< 2 nm) and mesopores (2-50 nm) in the sample.[29] From the isotherm, the calculated BET surface area was 231.57 m^2/g, a total pore volume was 0.69 cm^3/g, and an average pore diameter was 2.679 nm. In contrast, the BET surface area of commercial ZnO, ZnO (550N) and citric acid (550N) was only 5.91, 2.52 and 23.5 m^2/g, respectively. The decrease of BET surface area of ZnO (550N) compared to commercial ZnO might be due to a certain agglomeration of commercial ZnO particles under high calcined temperature. However, the increase of BET surface area of ZnO/C (550N) sample according to commercial ZnO and citric acid (550N) probably because of the ZnO particles could provide a platform to prevent the agglomeration of carbon particles which carbonized from citric acid.

Formation mechanism of ZnO/C composites

Based on the above results, we speculated a possible formation mechanism for the development of ZnO/C composites, as illustrated in Fig. 5. In the initial suspension, citric acid molecules distributed around the ZnO particles. After stirring, a large number of citric acid

molecules adsorbed onto the ZnO particles surface according to the electrostatic attraction and then the ZnO-citric acid precursor was obtained. Through calcination in N_2, citric acid was carbonized on the ZnO surface and the ZnO/C composites were obtained.

MB adsorption capacity of the products

Fig. 6 shows the MB adsorption capacities of the commercial ZnO, ZnO (550N), citric acid (550N) and ZnO/C (550N) samples. Adsorption-desorption equilibrium was reached with 30 min. It should be noted that the adsorption capacity of the ZnO/C (550N) product is much higher than that of commercial ZnO, ZnO (550N) and citric acid (550N) samples. This phenomenon is probably attributed to two main factors. First, the main driving force for dye adsorption by carbonaceous species is the interactions between the graphitic carbon layer (sp^2 bonding) and the aromatic rings of the dye molecules.[30] And Second, the BET surface area of ZnO/C (550N) composites (231.57 m^2/g) is much higher than commercial ZnO (5.91 m^2/g), ZnO (550N) (2.52 m^2/g) and citric acid (550N) (23.5 m^2/g) samples, which is also an important influential factor for adsorption capacity of the products.[31]

Photocatalytic decomposition activity of the products

The photocatalytic activities of the commercial ZnO, ZnO (550N), citric acid (550N) and ZnO/C (550N) were evaluated by measuring the decomposition of MB under UV irradiation. According to the Beer-Lambert law, the concentration of MB is linearly proportional to the intensity of the absorption peak at 664 nm, and thus the decomposition efficiency of MB can be calculated using the following expression:

$$\text{MB decomposition (\%)} = 100 \times (C_o - C) / C_o \quad (1)$$

Where, C_o and C are the equilibrium concentrations of MB before and after UV

irradiation, respectively. Fig. 7 (a) shows the photocatalytic decomposition of MB monitored according to the concentration change versus time for the various samples. As seen in Fig. 7 (a), the concentration of MB has no significant change with the existence of citric acid (550N) or without catalyst. However, after UV irradiation for 12 min, the degradation efficiency of MB is about 32, 33, and 98% for the commercial ZnO, ZnO (550N) and ZnO/C (550N), respectively. Obviously, the ZnO/C (550N) sample exhibits much higher photocatalytic activities than that of commercial ZnO, ZnO (550N) and citric acid (550N). Furthermore, to quantitatively understand the reaction kinetics of MB degradation over different samples in our experiments, we re-plotted the data in Fig. 7 (b) according to the pseudofirst-order kinetic model as expressed by equation (2), which is generally used for photocatalytic degradation process take place at the interface between the catalysts and the organic pollutants with low concentration.

$$\ln (C_o/C) = kt \qquad (2)$$

Where, t is reaction time, k is the rate constant, C_o and C are the concentrations of MB solution at time 0 and t, respectively. As can be seen, the psedudo-first-order rate constants for the photodegradation of MB under UV-light irradiation are 0.326 min^{-1}, 0.033 min^{-1}, 0.032 min^{-1} and 0.0009 min^{-1} with ZnO/C (550N), ZnO (550N), commercial ZnO, and citric acid (550N), respectively. Thus, the ZnO/C (550N) sample may provide great application for the elimination of organic pollutants from wastewater.

On the basis of the above results, a proposed mechanism was discussed to explain the enhancement of the photocatalytic properties of the ZnO/C composites as shown in Fig. 8 (a). The mechanism illustrated that the carbon particles were believed to exhibit cooperative or

synergetic effects between carbon particles and semiconductive metal oxides. Upon UV light irradiation, electrons (e^-) in the valence band of ZnO were excited to the conduction band with the simultaneous generation of holes (h^+) in the valence band, photogenerated electrons (e^-) in ZnO may move freely toward the surface of the carbon particles and excess of valence band holes (h^+) were left in the ZnO to migrate to the surface and reacted with H_2O or OH^- to produce active species such as OH·,[32] suggesting that the photogenerated electrons and holes were efficiently separated and the lifetime of the excited electrons and holes could be prolonged in the transfer process, inducing higher quantum efficiency, and thus the photocatalytic activity of ZnO/C composites were enhanced greatly. Furthermore, the separation of photogenerated electrons and holes in the ZnO/C composites were confirmed by PL emission spectra of ZnO (550N) and ZnO/C (550N) in Fig. 8 (b). As can be seen, the ZnO/C composites exhibited much lower emission intensity than that of ZnO (550N), indicating that the recombination of the photogenerated charge carrier was inhibited greatly in the ZnO/C composites. The efficient charge separation could increase the lifetime of the charge carriers and enhance the efficiency of the interfacial charge transfer to adsorbed substrates, accounting for the higher activity of the ZnO/C composites.[33] The mechanism for the photocatalytic degradation of MB in our experiment was proposed as follows:

$$\text{ZnO/C (550N)(s)} + h\nu \rightarrow \text{ZnO/C (550N)(s)} + e^- + h^+$$

$$e^- + O_2 \rightarrow O_2^{\cdot -}$$

$$O_2^{\cdot -} + H_2O \rightarrow HO_2\cdot + OH\cdot$$

$$HO_2\cdot + H_2O \rightarrow H_2O_2 + OH\cdot$$

$$H_2O_2 \rightarrow 2OH\cdot$$

$$h^+ + OH^- \rightarrow OH\cdot$$

$$OH\cdot + MB\ (dye) \rightarrow CO_2 + H_2O$$

$$h^+ + MB\ (dye) \rightarrow CO_2 + H_2O$$

Under UV light irradiation, photogenerated electrons (e^-) in ZnO moved freely to the surface of the carbon particles, meanwhile, the photogenerated holes (h^+) were left in the valence band of ZnO. The photogenerated electrons could be readily trapped by absorbed O_2 at the carbon particles surface or the dissolved oxygen to yield superoxide radical anions ($O_2\cdot^-$). Subsequently, $O_2\cdot^-$ was transformed into hydroperoxy radical ($HO_2\cdot$) and hydroxyl radical ($OH\cdot$), which was a strong oxidizing agent that can decompose the organic dye. Meanwhile, the photogenerated holes were trapped by surface hydroxyl groups (or H_2O) at the catalyst surface to yield hydroxyl radicals ($OH\cdot$), or directly trapped by organic pollutions for further oxidizing organic pollutants.

To evaluate whether the sample was suitable for practical applications, MB was added in different water sources to form several different MB solutions (30 mg/L), including tap water and river water collected from Changjiang River in China. Then, the different MB solutions were treated with the as-prepared ZnO/C (550N) sample followed the same adsorption and photocatalytic experiment process above and the results are shown in Fig. 9 (a) and (b). As can be seen, the ZnO/C (550N) sample almost behaved the same adsorption capacity and photocatalytic activity in different water sources, suggesting that this sample was suitable for removal of dyes from different water sources. It is indicate that the as-prepared ZnO/C (550N) composites have great potential application for pollution control in our environment.

Conclusion

In summary, ZnO/C composites were successfully synthesized via simple adsorption and calcination technique method with citric acid as carbon source. The crystallographic phase, morphology, and microstructure were characterized by XRD, EDS, SEM, TEM, TGA, and BET. The resultant materials showed excellent adsorbed capacity and photocatalytic activity with respect to MB solution than the pure ZnO, ZnO (550N) and citric acid (550N). Furthermore, ZnO/C (550N) composites could remove MB dye in different water sources like tap water and the Changjiang River water in China. And it is expected that the ZnO/C (550N) samples with high adsorbed capacity and photocatalytic activity will greatly promote their practical application to eliminate the organic pollutants from wastewater.

Acknowledgements

The authors are grateful to National Natural Science Foundation of China (Grant No.21106017 and 51077013), Fund Project for Transformation of Scientific and Technological Achievements of Jiangsu Province of China (Grant No. BA2011086), Specialized Research Fund for the Doctoral Program of Higher Education of China (Grant No.20100092120047) and Key Program for the Scientific Research Guiding Found of Basic Scientific Research Operation Expenditure of Southeast University(Grant No.3207042102)

References

1. J. M. Hall-Spencer, R. Rodolfo-Metalpa, S. Martin, E. Ransome, M. Fine, S. M. Turner, S. J. Rowley, D. Tedesco and M. C. Buia, *Nature*, 2008, **454**, 96-99.
2. M. A. Shannon, P. W. Bohn, M. Elimelech, J. G. Georgiadis, B. J. Marinas and A. M. Mayes, *Nature*, 2008, **452**, 301-310.
3. C. J. Vorosmarty, P. B. McIntyre, M. O. Gessner, D. Dudgeon, A. Prusevich, P. Green, S. Glidden, S. E. Bunn, C. A. Sullivan, C. R. Liermann and P. M. Davies, *Nature*, 2010, **468**, 334-334.
4. L. L. Li, Y. Chu, Y. Liu and L. H. Dong, *J. Phys. Chem. C*, 2007, **111**, 2123-2127.
5. H. B. Lu, S. M. Wang, L. Zhao, J. C. Li, B. H. Dong and Z. X. Xu, *J. Mater. Chem.*, 2011, **21**,

4228-4234.
6. S. S. Ma, R. Li, C. P. Lv, W. Xu and X. L. Gou, *J. Hazard. Mater.*, 2011, **192**, 730-740.
7. Y. R. Smith, A. Kar and V. Subramanian, *Ind. Eng. Chem. Res.*, 2009, **48**, 10268-10276.
8. L. S. Zhang, W. Z. Wang, J. O. Yang, Z. G. Chen, W. Q. Zhang, L. Zhou and S. W. Liu, *Appl. Catal. a-Gen*, 2006, **308**, 105-110.
9. S. J. Yang, J. H. Im, T. Kim, K. Lee and C. R. Park, *J. Hazard. Mater.*, 2011, **186**, 376-382.
10. S. Chakrabarti and B. K. Dutta, *J. Hazard. Mater.*, 2004, **112**, 269-278.
11. D. Li and H. Haneda, *Chemosphere*, 2003, **51**, 129-137.
12. J. L. Yang, S. J. An, W. I. Park, G. C. Yi and W. Choi, *Adv. Mater.*, 2004, **16**, 1661-1664.
13. H. B. Fu, T. G. Xu, S. B. Zhu and Y. F. Zhu, *Environ. Sci. Technol.*, 2008, **42**, 8064-8069.
14. R. Ostermann, D. Li, Y. D. Yin, J. T. McCann and Y. N. Xia, *Nano Lett.*, 2006, **6**, 1297-1302.
15. Y. Z. Chen, D. Q. Zeng, K. Zhang, A. L. Lu, L. S. Wang and D. L. Peng, *Nanoscale*, 2014, **6**, 874-881.
16. X. B. Cao, X. M. Lan, Y. Guo, C. Zhao, S. M. Han, J. Wang and Q. R. Zhao, *J. Phys. Chem. C*, 2007, **111**, 18958-18964.
17. K. S. Leschkies, R. Divakar, J. Basu, E. Enache-Pommer, J. E. Boercker, C. B. Carter, U. R. Kortshagen, D. J. Norris and E. S. Aydil, *Nano Lett.*, 2007, **7**, 1793-1798.
18. X. Wang, X. G. Kong, Y. Yu and H. Zhang, *J. Phys. Chem. C*, 2007, **111**, 3836-3841.
19. Y. H. Zheng, L. R. Zheng, Y. Y. Zhan, X. Y. Lin, Q. Zheng and K. M. Wei, *Inorg. Chem.*, 2007, **46**, 6980-6986.
20. I. Davidson, R. F. Silva, I. Davidson and L. M. Shutman, *Int. J. Infect. Dis.*, 2010, **14**, E459-E459.
21. S. Cho, J. W. Jang, J. S. Lee and K. H. Lee, *Crystengcomm*, 2010, **12**, 3929-3935.
22. Y. Guo, H. S. Wang, C. L. He, L. J. Qiu and X. B. Cao, *Langmuir*, 2009, **25**, 4678-4684.
23. J. B. Mu, C. L. Shao, Z. C. Guo, Z. Y. Zhang, M. Y. Zhang, P. Zhang, B. Chen and Y. C. Liu, *Acs Appl. Mater. Inter.*, 2011, **3**, 590-596.
24. T. S. Herng, S. P. Lau, L. Wang, B. C. Zhao, S. F. Yu, M. Tanemura, A. Akaike and K. S. Teng, *Appl. Phys. Lett.*, 2009, **95**, 012505-012505-3.
25. H. Pan, J. B. Yi, L. Shen, R. Q. Wu, J. H. Yang, J. Y. Lin, Y. P. Feng, J. Ding, L. H. Van and J. H. Yin, *Phys. Rev. Lett.*, 2007, **99**, 127201-127201-4.
26. S. T. Tan, X. W. Sun, Z. G. Yu, P. Wu, G. Q. Lo and D. L. Kwong, *Appl. Phys. Lett.*, 2007, **91**, 072101-072101-3.
27. D. Wyrzykowski, E. Hebanowska, G. Nowak-Wiczk, M. Makowski and L. Chmurzynski, *J. Therm. Anal. Calorim*, 2011, **104**, 731-735.
28. M. M. Barbooti and D. A. Alsammerrai, *Thermochim. Acta*, 1986, **98**, 119-126.
29. D. W. Wang, F. Li, M. Liu, G. Q. Lu and H. M. Cheng, *Angew. Chem. Int. Edit.*, 2008, **47**, 373-376.
30. Y. C. Hsu, H. C. Lin, C. W. Lue, Y. T. Liao and C. M. Yang, *Appl. Catal. B-Environ.*, 2009, **89**, 309-314.
31. H. S. Teng and C. T. Hsieh, *Ind. Eng. Chem. Res.*, 1998, **37**, 3618-3624.
32. Y. L. Wei, Y. F. Huang, J. H. Wu, M. Wang, C. S. Guo, Q. Dong, S. Yin and T. Sato, *J. Hazard. Mater.*, 2013, **248**, 202-210.
33. C. L. Yu, K. Yang, Y. Xie, Q. Z. Fan, J. C. Yu, Q. Shu and C. Y. Wang, *Nanoscale,* 2013, **5**, 2142-2151.

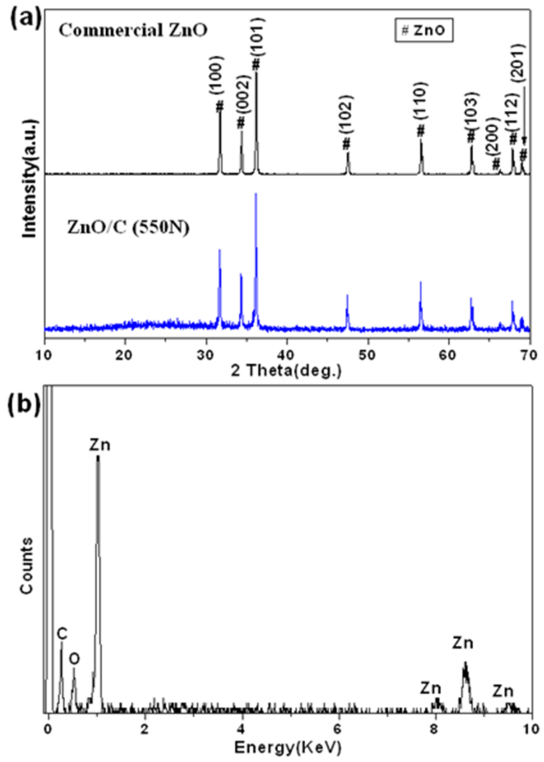

Fig. 1. XRD patterns of (a) commercial ZnO and ZnO/C (550N), and EDS spectrum (b) of the ZnO/C (550N).

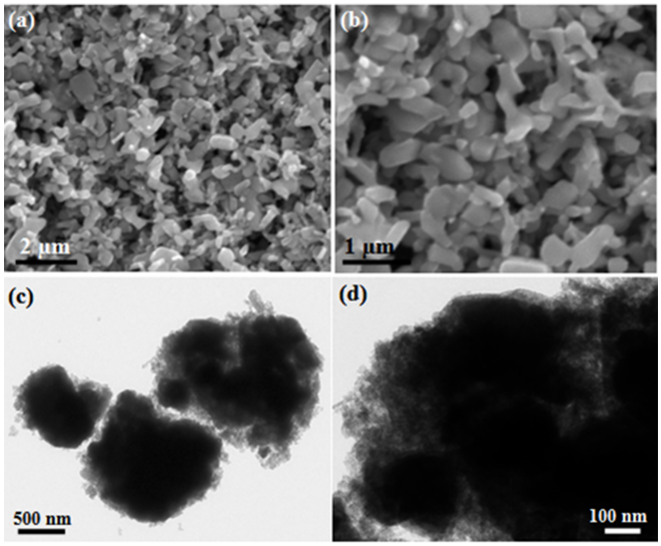

Fig. 2. (a, b) SEM and (c, d) TEM images of the ZnO/C (550N) sample with low and high magnifications.

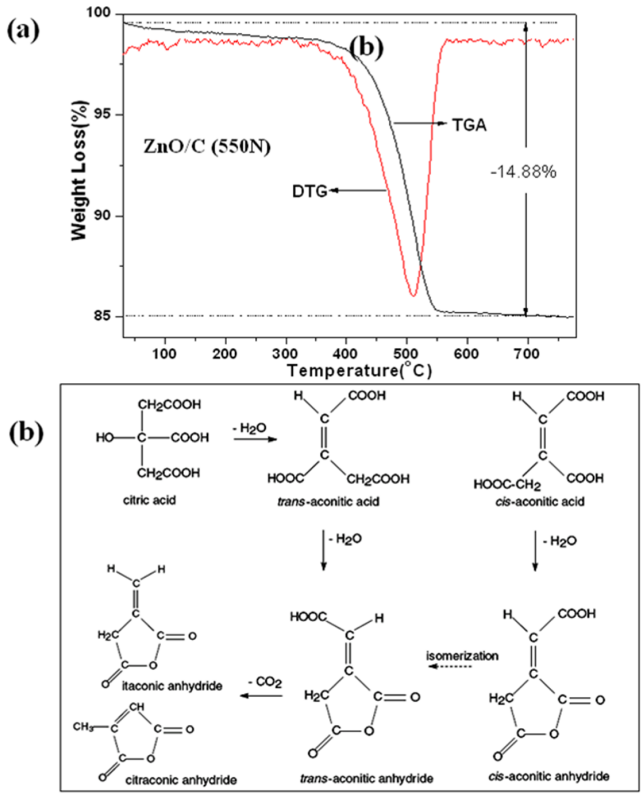

Fig. 3. TGA curves of (a) ZnO/C (550N), and (b) thermal transformations of citric acid.

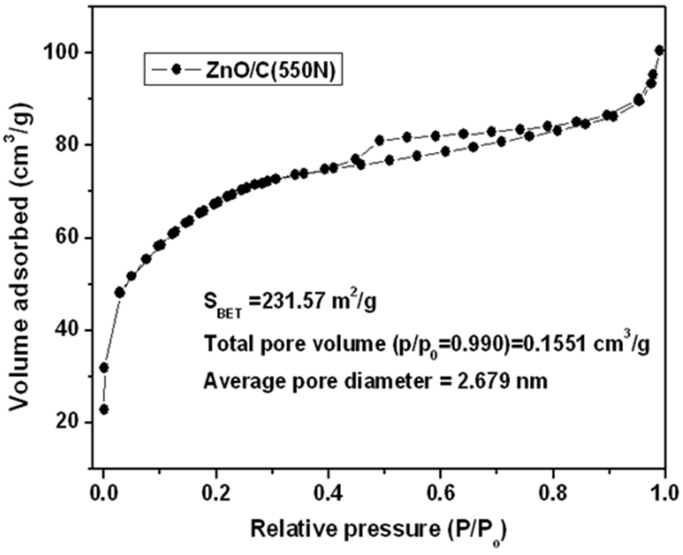

Fig. 4. N_2 adsorption-desorption isotherm of ZnO/C (550N).

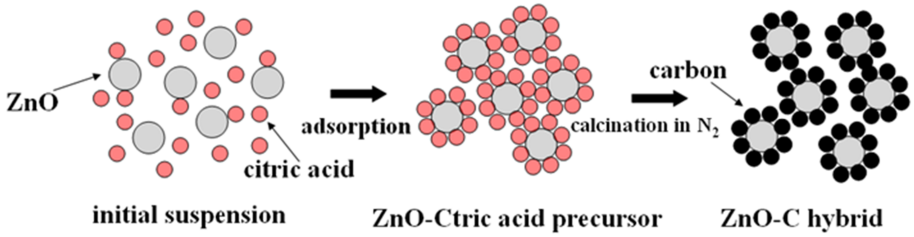

Fig. 5. Schematic illustration of a speculated formation mechanism of ZnO/C composites.

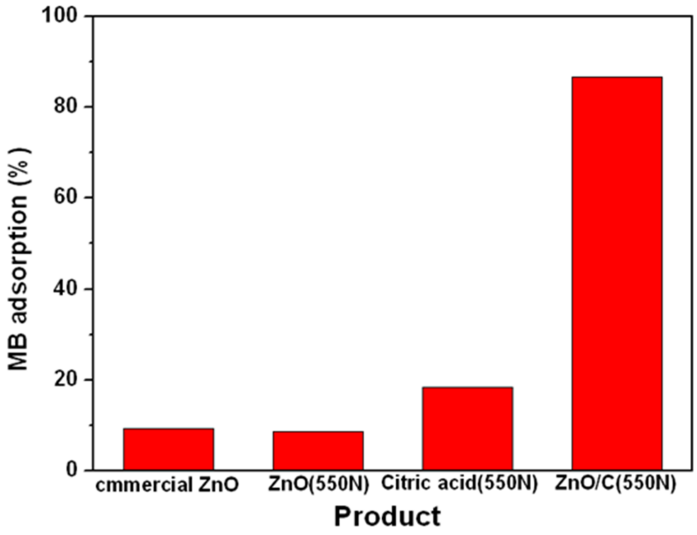

Fig. 6. MB adsorption capacities of commercial ZnO, ZnO (550N), citric acid (550N) and ZnO/C (550N) samples.

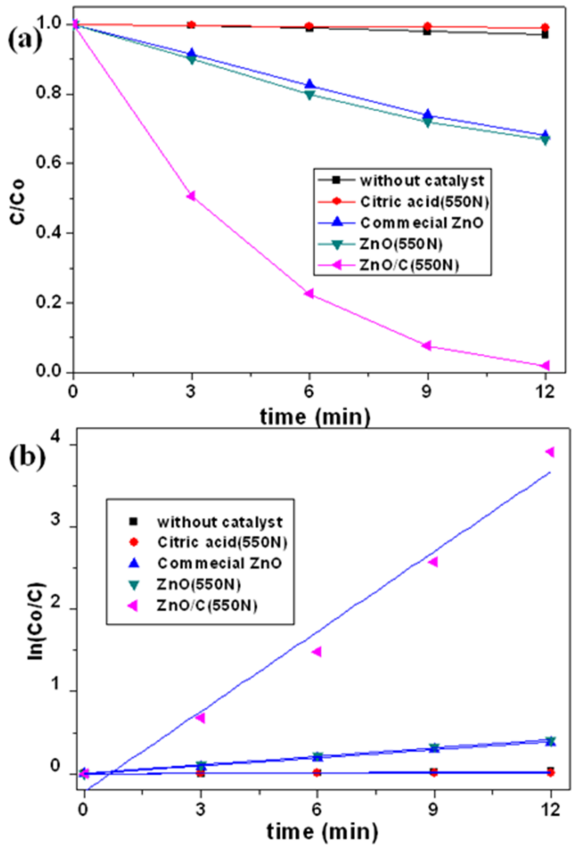

Fig. 7. (a) Photodegradation curves of MB as a function of UV irradiation time in the presence of catalysts (commercial ZnO, ZnO (550N), citric acid (550N) and ZnO/C (550N)). (b) the selected fitting results using the

pseudo-first-order reaction correspond to (a).

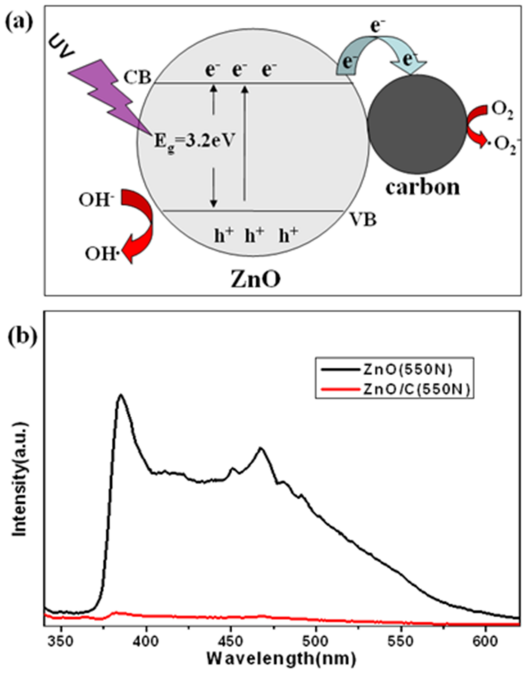

Fig. 8. (a) Proposed mechanisms for the photocatalysis of the ZnO/C (550N) composites. (b) PL emission spectra of ZnO (550N) and ZnO/C (550N).

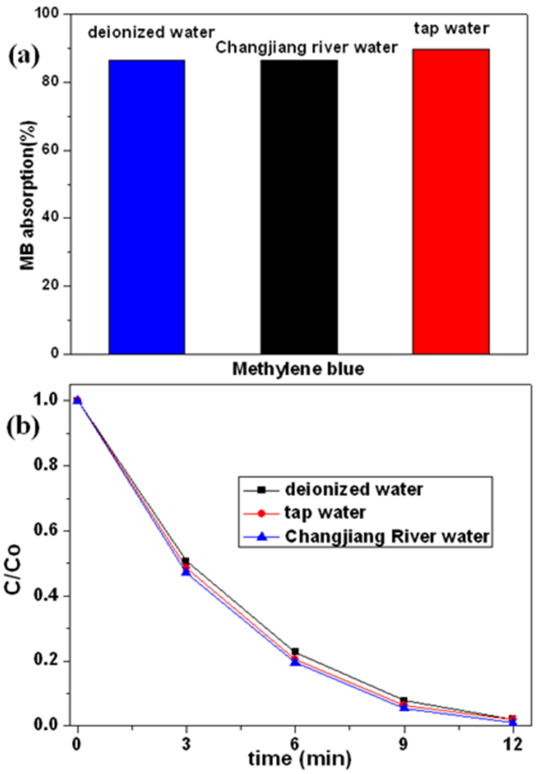

Fig. 9. MB adsorption capacities (a) and photocatalytic activity (b) of ZnO/C (550N) sample in different water source.